Highlights

• Aliphatic hyper-branched polycarbonate (HBPC) was synthesized by polycondensation.

• HBPC films containing $LiClO_4$ were evaluated as solid polymer electrolytes (SPEs).

• The Li ion conductivities were compared with that of linear polycarbonate-based SPE.

• The SPEs showed relatively high ionic conductivity and low activation energy.

• Introduction of branched structure is effective for the lithium ion transport.

Graphical abstract

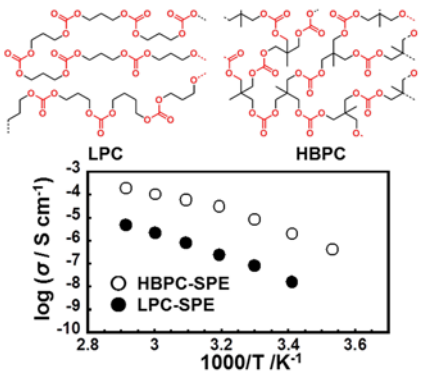

For original research paper in *Polymer*

Synthesis of an Aliphatic Hyper-branched Polycarbonate and Determination of its Physical Properties for Solid Polymer Electrolyte Use

Suguru Motokucho,[a,*] Hirotoshi Yamada,[a] Yusuke Suga,[a] Hiroshi Morikawa,[b] Hisayuki Nakatani,[a] Kouki Urita,[a] Isamu Moriguchi[a]

[a]Chemistry and Material Engineering Program, Nagasaki University, 1-14, Bunkyo-Machi, Nagasaki City, Nagasaki, 852-8521, Japan

[b]Department of Applied Chemistry, Kanagawa Institute of Technology, 1030, Shimo-ogino, Atsugi, Kanagawa 243-0292, Japan

*Corresponding author. E-mail: (motoku@nagasai-u.ac.jp)

Abstract

An aliphatic hyper-branched polycarbonate (HBPC) was synthesized as a novel host material for solid polymer electrolytes (SPEs). The HBPC was synthesized through $A_2 + B_3$ polymerization to yield a branched polycarbonate structure. HBPC-based SPE films were prepared by drying mixed solutions of HBPC and 1–60 mol% $LiClO_4$. The temperatures for 5% weight loss (T_{d5}s) of the HBPC-based SPEs were in the range of 174.4–189.3 °C, higher than those in normal use. The HBPC-based SPE exhibited higher ionic conductivities (1.86×10^{-4} S·cm^{-1} at 70 °C and 8.52×10^{-6} S·cm^{-1} at 30 °C) than a poly(trimethylene carbonate) (LPC)-based SPE (4.79×10^{-6} S·cm^{-1} at 70 °C and 8.32×10^{-8} S·cm^{-1} at 30 °C) for 20 mol% lithium content. Activation energies of lithium ion transport for the HBPC- and LPC-based SPEs were estimated to be 11.47 and 15.88 kJ·mol^{-1}, respectively. Introduction of this branched structure in polycarbonates is effective for promoting lithium ion transport.

1. Introduction

Current liquid electrolytes for lithium ion batteries consist primarily of organic carbonate compounds such as ethylene carbonate [1]. Liquid electrolytes show good solubilization for lithium salts and have low solution viscosity. Owing to these favorable properties, such a mixture of carbonate compounds can facilitate ion transport. As an important factor for the use of carbonate compounds in electrolytes, any mixture of carbonate compounds must show good interfacial compatibility at both the anode and cathode. However, these carbonate components are often flammable and can undergo volume expansion via volatilization, leading to serious explosion hazards during battery use [2–5].

Solid polymer electrolytes (SPEs) are a potential alternative material to solve these problems. Compared with liquid electrolytes, solvent-free SPEs are non-volatile, lightweight, and have good mechanical stability. Ionic conductivity by SPEs consisting of poly(ethylene oxide) (PEO) with metal salts was first reported by Wright and co-workers in 1973 [6]. Following this report, many researchers have attempted and reported improvement of their chemical and physical properties. To develop solvent-free SPEs with high ionic conductivity, many strategies, including synthesizing co-polyethers and comb-like polyethers, [7] composites with metal fillers [8], and hyper-branched polyethers [9,10], have been extensively studied.

It is well known that PEO-based SPEs have good ionic conductivities, exceeding 10^{-4} $S \cdot cm^{-1}$ at low salt concentrations. However, at high salt concentrations, cross-linking structures are usually formed in PEO-based SPEs, based on strong ionic interactions between the cations (e.g., lithium cations) and polar ether oxygens of the PEOs [11]. Hence, these PEO-based SPEs do not show enough ionic conductivity (over 10^{-3} $S \cdot cm^{-1}$ is required at room temperature) relative to most liquid or ceramic electrolytes. Recently, polymers with the same structures as liquid electrolytes (carbonate compounds), such as polycarbonates, have attracted much attention because of their promising potential as SPEs. Several linear

polycarbonates have been synthesized for the development of high-ionic-conductivity SPEs using polycarbonates [12–24]. For example, Shriver and Wei used poly(vinylene carbonate) as an SPE [12]. Smith and Brandell and their respective co-workers reported poly(trimethylene carbonate) [13–16]. Tominaga and co-workers reported poly(ethylene carbonate) derivatives for use in SPEs [17–22]. The poly(ethylene carbonate)s have carbonate groups in their polymer backbones and show relatively high ionic conductivities in the presence of lithium salts. Poly(ethylene carbonate) with ether side chains showed an extremely high lithium ion transference number (more than 0.7) [17]. Matsumoto and co-workers reported polycarbosilanes with a cyclic carbonate group on the side chain [23,24]; these polycarbosilane-based SPEs had excellent thermal, chemical, and electrochemical properties. These reports suggest that polymers with carbonate structures are promising SPEs, exhibiting high ionic conductivities. Previous studies on polycarbonate-based SPEs have shown that the ionic conductivity increases as the molecular flexibility of the local structure in the polymer increases. Therefore, it is important that flexible groups are introduced into the polymer backbone [15,19,24], which can lower the glass transition temperature (T_g) and activation energy, or enhance the number of carrier ions. Elsewhere, Behera *et al*. reported that hyper-branched polyesters consistently have lower T_g values than those of their linear analogues bearing the same monomeric units [25]. It is well known that the activation energy of the molecular motion of a polymer chain [26,27], as well as its T_g, generally decreases owing to the introduction of hyper-branched structures into the polymer backbone.

Taking into account the relationship between ion conduction capabilities, flexible or branched structures, and the effectiveness of carbonate moieties, it is expected that the introduction of a hyper-branched structure into polycarbonates would be a promising way to produce innovative SPEs. In this work, we present our initial study on SPEs consisting of a hyper-branched polycarbonate (HBPC) with lithium perchlorate ($LiClO_4$) contents of 1, 5, 20, 40, and 60 mol%. For this purpose, we synthesized an aliphatic HBPC by simple

polycondensation employing an organic base, 1,8-diazabicyclo[5.4.0]undec-7-ene, as a catalyst. Its applicability as an SPE was demonstrated.

2. Experimental Section

2.1. Materials

All chemicals were purchased from WAKO Chemicals Co., Ltd. Trimethylolethane (TME) and $LiClO_4$ were dried *in vacuo* at 80 °C for 24 h prior to use. Dimethylcarbonate (DMC) was distilled under nitrogen. 1,8-Diazabicyclo[5.4.0]undec-7-ene (DBU) was distilled under reduced pressure. Linear-type poly(trimethylene carbonate) (LPC, M_n = 2,000) was supplied by ASAHI KASEI Chemicals, Co., Ltd.

2.2. Characterization

2.2.1 ^{1}H and ^{13}C nuclear magnetic resonance (NMR) spectroscopy

HBPC was characterized by ^{1}H and ^{13}C NMR spectroscopy (JNM-GX400, JEOL Co. Ltd., Japan) with tetramethylsilane (TMS) as an internal standard.

2.2.2 Gel permeation chromatography (GPC) analysis

The number-average and weight-average molecular weights (M_n and M_w, respectively) and polydispersity ($Đ_M$) were determined by GPC on a column containing shim-pack GPC-80M (SHIMADZU Co. Ltd, Japan) at 40 °C, using a JASCO PU 2060 pump system equipped with a JASCO RI 1530 refractive index detector, with tetrahydrofuran as an eluent at a flow rate of 1.0 mL·min^{-1}. M_n, M_w, and $Đ_M$ were calibrated with polystyrene standards.

2.2.3 Differential scanning calorimetry (DSC) measurements

DSC curves of HBPC and HBPC-based SPEs were obtained on a SHIMADZU DSC-60 Plus. Samples (5 mg) were sealed in aluminum pans, and measurements were carried out at a heating rate of 10 °C·min^{-1} over the range of −100 to 150 °C under nitrogen.

2.2.4 Thermogravimetric analysis (TGA)

TGA measurements were performed with a SHIMADZU DTG-60. Samples (5 mg) were weighed in aluminum pans, and sample measurements were carried out at a heating rate of 10 °C·min^{-1} in dried air. The sample weight loss was then recorded.

2.2.5 Fourier-transform infrared (FT-IR) analysis

IR spectra of the samples were measured with an FT-IR spectrometer (Thermo Nicolet NEXUS670 FTIR) with an attenuated total reflection option. Measurements were carried out at room temperature with 32 scans at a resolution of 4 cm^{-1} over the full mid-IR range (800–4000 cm^{-1}).

2.3. Preparation and measurements of samples

2.3.1 Preparation of HBPC

In a 300 mL flask equipped with a Dean-Stark receiver, a white solid mixture consisting of TME (24.03 g, 200.0 mmol) and DBU (0.91 g, 6.0 mmol) was dissolved in DMC (25.3 mL, 27.02 g, 300.0 mmol) at room temperature. The mixture was heated to 78 °C, and stirred at this temperature until methanol was removed (20 d). The resulting reaction mixture was concentrated under reduced pressure to yield a colorless transparent syrup. The obtained syrup was purified by precipitation from diethyl ether. The obtained colorless syrup was dried *in vacuo* to yield 26.3 g HBPC as a colorless waxy solid. The HBPC showed good solubility in toluene, chloroform, acetonitrile, and tetrahydrofuran, and was insoluble in methanol and water. The waxy solid was characterized by ^{1}H and ^{13}C NMR, FT-IR, and GPC.

^{1}H NMR (400 MHz, DMSO-d_6) δ: 0.79 (*R*), 0.87 (*Q*) and 0.95 (*P*) (–C*H*$_3$), 3.25 (*r*) and 3.28–3.29 (*s*) (–C*H*$_2$OH), 3.67–3.70 (*A*, *a*) (–O(C=O)O–C*H*$_3$), 3.97–4.00 (*q*), 4.04–4.06 (*p*) (–C*H*$_2$O–) 4.52–4.55 and 4.83–4.85 (*B* and *b*) (–O*H*) ppm.

^{13}C NMR (100 MHz, DMSO-d_6) δ: 15.99 (*R*), 16.03 (*Q*) and 16.15 (*P*) (–*C*H$_3$), 38.47, 38.53, 38.58 (*O*, quaternary carbon), 54.64 (*A*), 54.80 (*a*) (–O*C*H$_3$), 62.65 (*s*), 63.24 (*r*) (–*C*H$_2$OH),

68.69–68.91 (*q*), 69.23–69.49 (*p*), 154.22, 154.42, 154.61, 154.91, 154.93 and 155.14 (*C*, *C*=O) ppm. [These chemical shifts were assigned from ref. 28.]

IR (KBr) 2935, 2857 (ν (C–H)), 1755 and 1743 (ν (C=O)) cm^{-1}, T_g = −20.1 °C. The M_n and $Đ_M$ values are 2,500 and 1.33, respectively.

2.3.2 Preparation of solid polymer electrolytes

SPEs were prepared from HBPC and anhydrous $LiClO_4$ in a glove box under argon. Stoichiometric amounts of $LiClO_4$ and HBPC were dissolved in anhydrous acetonitrile to form a highly viscous homogeneous solution. The viscous solution was cast on a polytetrafluoroethylene plate, and the solvent was evaporated at room temperature in the glove box for several hours and then under high vacuum for 18 h to obtain a homogeneous and flat film. The SPE film samples (abbreviated as HBPC-based SPEs) were distinguished by the molar ratio of the lithium cations (Li^+) to carbonate moieties in the HBPC; [Li^+]/[carbonate] = 1, 5, 20, 40, or 60 mol%. As a reference, an LPC-based SPE containing 20 mol% $LiClO_4$ was prepared by the same method.

2.3.3 Ionic conductivity

AC impedance measurements of HBPC-based SPEs were carried out with a frequency analyzer (Solartron 1260). The test cell consisted of an SPE sample with 80-μm-thick polyethylene films as spacers sandwiched between two gold-vapor-deposited (1.0 cm^2) glasses. All SPEs were analyzed within a temperature range of 10–70 °C, over a frequency range of 10 Hz to 1 MHz with an amplitude of 10 mV. The SPE resistance was obtained from Nyquist plots by fitting the high-frequency semicircle and/or the low-frequency linear response to appropriate equivalent circuits using ZView (Scribner Associates Inc.). The ionic conductivity for the SPE was calculated as

$$\sigma = t/GR \qquad (1)$$

where t is the SPE film thickness (80 μm), G is the gold-vapor-deposited area (1.0 cm^2), and R is the SPE film resistance.

3. Results and Discussion

3.1. Synthesis of hyper-branched polycarbonate

Previously, condensation reactions of diols with DMC have been used to prepare organic polycarbonates with linear structures. Very recently, polycarbonates with branched structures were also synthesized [28]. In that article, a triol and DMC were condensed in the presence of lithium acetylacetonate in dioxane under refluxing conditions. However, large amounts of molecular sieves (4Å) were also used to remove the resulting methanol. It is likely that the reaction is sensitive to the activity of the molecular sieves, which depends on the moisture. Furthermore, the researchers reported that the condensation mixture set to a gel without solvents and was carried out in dioxane solution to prevent such gelation. Generally, it is required for the preparation of SPEs that the desired polymers are simply prepared on a large scale. Here, therefore, we selected a facile HBPC synthesis that involved receiving the produced methanol in a Dean-Stark receiver without any solvents.

HBPC was synthesized via the polycondensation of the two bi- and tri-functional monomers, DMC and TME, known as $A_2 + B_3$ polycondensation [28–32], as shown in Scheme 1a. The reaction proceeded slowly in the presence of a catalytic amount of DBU and was stopped after methanol from the reaction mixture was completely distilled. The reaction did not lead to gelation without solvents in our study, although it set into gel without solvents in a previous study [28]. The obtained crude product was purified by precipitation into diethyl ether to yield HBPC as a colorless waxy solid.

The M_n and $Đ_M$ of HBPC are 2,500 and 1.33, respectively. A unimodal peak is observed in the GPC profile (Fig. 1). In the FT-IR spectrum of HBPC, characteristic absorbance bands

are present near 1750 (1743 and 1755) cm^{-1}, which can be assigned to carbonyl groups of the carbonate esters.

The ^{1}H NMR spectrum of HBPC is shown in Fig. 2a. All signals are listed and characterized in the experimental section. Six kinds of partial units, dendritic units (D), terminal units (T^1, T^2), and linear units (L^1, L^2, L^3), in HBPC are also depicted in Fig. 2. The three singlet signals observed at 0.79, 0.87, and 0.95 ppm are ascribed to methyl protons neighboring the quaternary carbon atoms in the HBPC [28]. The ^{1}H NMR signals corresponding to the dendritic, terminal, and linear (D, T^1, L^1 in Fig. 2) units overlap at the same chemical shifts (*P* and *p* at 0.95 and 4.04–4.06 ppm, respectively). On the other hand, there are two minor signals at 3.25 (*r*) and 3.28–3.29 (*s*) ppm in addition to the major signals (*A* and *a*) at 3.67–3.70 ppm. These minor signals are ascribed to methylene protons on the hydroxymethyl groups (*r* and *s*) in the L^2, T^2, and T^3 units. Obviously, there are both hydroxy groups and carbonate moieties at the terminal moieties in HBPC. On the basis of the integrated intensities of the set of signals at 3.67–3.70 ppm (*A* and *a*) and 3.25 and 3.28–3.29 ppm (*r* and *s*), the ratio [–O–CO–OCH_3]:[–CH_2-OH] at the termini is found to be 79:21, meaning that the termini feature 79% carbonate units and 21% hydroxy units. This differs somewhat from values determined in a previous study [28], in which approximately 70% hydroxy units were present.

The ^{13}C NMR spectrum of HBPC is shown in Fig. 2b. Each set of signals was assigned as shown in Fig. 2b and in the experimental section. The six signals at approximately 155 ppm are derived from the carbonyl carbon atoms in the dendritic, terminal, and linear units. In addition, a set of three signals appears at 15.99, 16.03, and 16.15 ppm, which are assigned to carbon atoms on the three kinds of methyl groups (*P*, *Q*, and *R* in Fig. 2). Based on these IR, NMR, and GPC results, the obtained HBPC is determined to have a branched structure and a moderate molecular weight.

3.2 Polycondensation behavior

To clarify the condensation behavior of TME and DMC to yield HBPC, the reaction mixture was analyzed by ^{1}H NMR. The feed molar ratio of TME and DMC was adjusted to [–CH_2OH]:[carbonate]=2:1, and the temperature was 78 °C. Here, we investigate the condensation behavior in terms of TME consumption and the three compositions of tri-, di-, and monocarbonate units (*P*, *Q*, and *R* in Fig. S1), which are classified into the partial structures D, L, and T in Fig. 2.

As shown in Fig. S1, a set of characteristic singlet signals is observed near 1 ppm. On the basis of the HBPC assignments (Fig. 2), the three signals at 0.79, 0.87, and 0.92 ppm are characterized as the methyl protons *P*, *Q,* and *R*, respectively, derived from the sequential reactions of the TME-derived units with the DMC monomer to form tricarbonate, dicarbonate, and monocarbonate units or carbonate species. The degree of carbonation is in the order of *P* > *Q* > *R* units. For example, the diol unit *R* is a reaction product of TME with only one carbonate component. Besides these, a signal due to the starting TME is also present at 0.71 ppm (Fig. S1). From the integrated values of the four methyl group signals, the actual mole composition of the units (*P*, *Q,* and *R*) in the reaction mixture was estimated.

At first, the condensation of TME and DMC was carried out without a Dean-Stark receiver, as the vessel containing the reaction mixture was sealed to prevent the evaporation of methanol from the reaction. Figure 3a shows the time-course plots of both the conversion of the starting TME and the mole composition of the three units, *P*, *Q*, and *R*. The conversion of TME exhibits a plateau value of *ca*. 80% over the examined range, and quantitative conversion is not observed even after 136 h, meaning significant amounts of the starting compounds remain. After 136 h, the *P*, *Q*, and *R* unit compositions are 13, 25, and 44%, respectively. Clearly, the tricarbonate unit composition (*P*) was low in contrast to the high content of the monocarbonate unit (*R*). This indicates the condensation reaction did not proceed sufficiently.

On the other hand, the reaction behavior changes drastically when the methanol by-product is collected as a distillate with a Dean-Stark receiver. As shown in Fig. 3b, the quantitative consumption of TME is achieved after 6 h reaction. The content of the monocarbonate unit *R* decreases remarkably within 48 h, and decreases gradually with increasing reaction time to almost negligible values. As the contents of the dicarbonate and monocarbonate units *Q* and *R* decrease, the amount of the tricarbonate unit *P* increases gradually, reaching 60% and more beyond 300 h, suggesting the formation of a branched structure such as HBPC.

The results in Fig. 3a and 3b indicate that the polycondensation of TME and DMC is an equilibrium reaction between the methanol and carbonate components. Therefore, collecting methanol as a distillate is important for the formation of HBPC. Furthermore, this polycondensation does not set into a gel presumably because a small amount of DMC is evaporated from the reaction mixture into the receiver, deviating the feed ratio of [–CH_2OH]:[carbonate].

3.3. Films of HBPC-based SPEs

Film samples of HBPC-based SPEs for use as practical polyelectrolytes were prepared by mixing the prepared HBPC and predetermined amounts of $LiClO_4$ (1, 5, 20, 40, and 60 mol%), followed by casting and drying, which yielded HBPC-based SPE films containing known lithium ion contents. A sample of only HBPC (no $LiClO_4$) was dried in the same manner as the HBPC-SPEs; however, a waxy solid was obtained instead of a film. The HBPC-based SPE containing 20 mol% $LiClO_4$ is a rubbery, homogeneous, semitransparent, and self-standing film (left image, Fig. 4). The film with 40 mol% $LiClO_4$ (middle, Fig. 4) is rubbery and partially opaque. When the addition of $LiClO_4$ is increased to 60 mol%, the resulting HBPC-based SPE becomes a hard and considerably opaque film (right, Fig. 4). This opacity may arise from the aggregation of lithium salts in the films, in which the 40 or 60 mol%

$LiClO_4$ in the SPEs is not dispersed and forms immiscible microstructures. These results suggest that adding excess amounts of lithium salt into the HBPC is not appropriate for SPE film preparation.

3.4. Thermal and IR analyses

Because SPEs are practically incorporated in working batteries, the investigation of their thermal properties is meaningful. Hence, the thermal properties of both the original HBPC and the prepared HBPC-based SPEs were analyzed by DSC (Fig. 5a) and TGA (Table 1). The T_g values of the HBPC and HBPC-based SPEs are observed in the range of −20.1 to −9.4 °C. These values are much lower than room temperature, indicating that unexpected phase transitions will not occur when the SPEs are used at room temperature. The T_g values gradually increase as the $LiClO_4$ content increases, indicating the existence of interactions between the lithium cations and carbonyl groups of the carbonate moieties in HBPC. Similar behavior associated with T_g increment was previously reported for SPEs made from LPCs and lithium salts [13]. In the HBPC-based SPEs containing 40 and 60 mol% $LiClO_4$, endothermic peaks appear at temperatures over 60 °C. These peaks may arise from the uncomplexed lithium salts that were not dispersed in the SPEs. This idea is consistent with the opacities of the films containing 40 or 60 mol% $LiClO_4$ (Fig. 4).

The thermal stabilities of the original HBPC and HBPC-based SPEs were measured by TGA. The 5% weight loss temperatures (T_{d5}s) of the original HBPC and HBPC-based SPEs are listed in Table 1. The T_{d5} of HBPC is 163.5 °C; this value increases with the addition of $LiClO_4$ to HBPC. The T_{d5} temperatures for the SPEs are in the range of 174.4–189.3 °C, higher than those in normal use [13]. In the previous study [13], it was reported that temperatures higher than 160 °C would be acceptable in case of thermal runaway in the battery. Therefore, our HBPC-SPEs might temporarily withstand such an event. However, their thermal stability should be improved for practical use.

Figure 5b shows the FT-IR spectra of the HBPC and HBPC-based SPEs in the region from 1500 to 1900 cm^{-1}. Two peaks around 1750 cm^{-1} can be identified as stretching vibrations of the carbonyl (C=O) groups in the main chain (–CH_2O(C=O)–OCH_2–) and terminal groups (–CH_2O(C=O)–OMe) of HBPC. There is a significant change in the spectra between the original HBPC and the SPEs. A new peak at 1725 cm^{-1} clearly appears, which increases in intensity as $LiClO_4$ is added, whereas the peak around 1750 cm^{-1} decreases in turn. The coordination of metal ions to C=O groups decreases their electron density, resulting in the new peak that appears at lower wavenumber [33,34]. These observations clearly indicate strong interactions between the carbonate carbonyl groups in the polymers and the added lithium cations. The same IR absorption shift phenomenon has been reported by other research groups [15,21,24]. This evidence of the interaction between the lithium cations and carbonyl groups based on FT-IR data also explains the DSC results (Fig. 5a), namely, the increase in T_g with increasing $LiClO_4$ content. Presumably, the coordination of lithium cations to the carbonyl groups decreases the relaxation of the polymer chains, leading to the increased T_g values.

3.5. Impedance measurements

To clarify the effect of branching structures on the improvement in the ionic conductivity, LPC was used as a contrast to HBPC owing to its linear structure (Scheme 1b). Figure 6a depicts the temperature dependence of the ionic conductivity σ ($S \cdot cm^{-1}$) of the HBPC-based SPEs, plotted against the reciprocal of absolute temperature as an Arrhenius plot. A second horizontal axis, giving the temperature in Celsius, is included for comprehensibility. In all samples, the conductivity increases as the reciprocal temperature decreases; higher values are obtained at higher temperatures. In the HBPC-based SPEs with 1–20 mol% $LiClO_4$, the ionic conductivities show an upward-convex curve, indicating Vogel-Tammann-Fulcher (VTF) behavior [35]. These results suggest that the SPEs are amorphous at lithium contents of 1–20

mol%. This interpretation agrees with the absence of melting endotherms in the DSC experiments (Fig. 5a). Among the samples with 1–20 mol% $LiClO_4$, the HBPC-based SPE with 20 mol% $LiClO_4$ content shows the highest ionic conductivity at almost all examined temperatures. On the other hand, for the 40 or 60 mol% $LiClO_4$-containing HBPC-based SPEs, the ionic conductivities have inflection points near 50 °C. At this temperature, endothermic peaks are observed in the DSC charts (Fig. 5a). Therefore, this inflection presumably arises from the fusion of uncomplexed salts or other similar species.

The ionic conductivities of LPC-based and HBPC-based SPEs were compared at a fixed $LiClO_4$ content of 20 mol% (Fig. 6a). The conductivities for the LPC-based SPE are 4.79×10^{-6} S·cm^{-1} at 70 °C and 8.32×10^{-8} S·cm^{-1} at 30 °C. The conductivities of the HBPC-based SPEs are 1.86×10^{-4} S·cm^{-1} at 70 °C and 8.52×10^{-6} S·cm^{-1} at 30 °C. The conductivities of the HBPC-based SPEs are higher than those of the LPC-based ones at the same temperature. These results clearly indicate that the introduction of hyper-branched structures has a positive effect on the ionic conductivity of SPEs, most likely because of the lower activation energy for ion transport in the hyper-branched structure compared to the linear. Moreover, the conductivity obtained from the HBPC-based SPEs reaches relatively high values compared with other polycarbonate-based SPEs containing $LiClO_4$ [13,17,19].

The activation energies of each polymer matrix (HBPC and LPC) were also estimated. The temperature dependence of the ionic conductivity is expressed by the following VTF equation (2):

$$\sigma = \frac{A}{T^{1/2}} \exp\left[-\frac{E_a}{\mathrm{R}(T-T_o)}\right] \qquad (2)$$

where A ($K^{1/2}$ S·cm^{-1}) is a constant that is proportional to the number of carrier ions and T is the absolute temperature (283.15–343.15 K (10–70 °C)) of the measurement. T_0 is the temperature at which the free volume vanishes (ideal T_g), R (J·mol^{-1}·K^{-1}) is the fundamental gas constant, and E_a (kJ·mol^{-1}) is the activation energy for ionic transport via segmental motion [36]. Equation (2) can be rewritten in logarithmic form as follows:

$$\ln\left(\sigma \cdot T^{1/2}\right) = -\frac{E_a}{\mathrm{R}(T-T_o)} + \ln A \qquad (3).$$

A and E_a can be estimated from the intercept and gradient of each linear plot based on Eq. (3). Using Eq. (3), VTF plots of HBPC-based SPEs (1–20 mol% $LiClO_4$) and LPC-based SPE (20 mol% $LiClO_4$) are shown in Fig. 6b. The plots for HBPC-based SPEs with 40 or 60 mol% $LiClO_4$ are omitted because their curves deviate from linearity, presumably due to the fusion of uncomplexed salts or other similar species. To ensure a root mean square error close to 1.0 (>0.99) in each plot made using Eq. (3), we take T_0 to be 50 °C lower than T_g. The E_a values of each SPE were calculated from the slopes of the three plots given in Fig. 6b. The values of E_a of the HBPC-based SPEs are almost constant, suggesting that the conduction mechanism does not change even as the salt concentration increases over 1–20 mol% $LiClO_4$. The E_a value for the LPC-based SPE is 15.88 kJ·mol^{-1}. Surprisingly, the values of HBPC-based SPEs are approximately 11 kJ·mol^{-1} (10.97, 11.01, and 11.47 kJ·mol^{-1} for 1, 5, and 20 mol% $LiClO_4$, respectively), much lower than that of the E_a value of the LPC-based SPE. This comparison indicates that the branched structure is also effective for the ion conduction of lithium salts among polycarbonate-based SPEs, which may arise from the high density of carbonate groups in HBPC that these structures can afford.

4. Conclusions

A hyper-branched aliphatic polycarbonate (HBPC; M_n = 2,500) was synthesized, and HBPC-based SPEs containing 1–60 mol% $LiClO_4$ were prepared as films. At 20 mol% lithium salt content, the ionic conductivity of the HBPC-based SPE reached its maximum values of 1.86 × 10^{-4} S·cm^{-1} at 70 °C and 8.52 × 10^{-6} S·cm^{-1} at 30 °C. These values were much higher than those of the LPC-based SPE at the same lithium ion content. Activation energies for ionic transport in the HBPC-based and LPC-based SPEs were also calculated from Vogel-Tammann-Fulcher plots as approximately 11 and 15.88 kJ·mol^{-1}, respectively.

Based on these data, introducing branched structures into the polycarbonate matrix is a promising approach for the development of SPEs with high ionic conductivity.

A study on the properties and performance of HBPCs in combination with other Li salts is in progress in our laboratory.

Acknowledgements

We thank Dr. Tetsuo Masubuchi, Mr. Hayato Yabuki, and Mr. Yasufumi Kawai of Asahi Kasei Chemicals, Co., Ltd., for providing poly(trimethylene carbonate). This study made use of SHIMADZU DSC-60 Plus and SHIMADZU DTG-60 instruments in the Advanced Material Science Research Unit Sharing System of Nagasaki University.

Funding: This work was supported by the Ministry of Education, Culture, Sports, Science and Technology [KAKENHI Grant-in-Aid for Scientific Research (C), No. 17K06000] and the Iwatani Naoji Foundation [Research Grant No. 15-4223].

Keywords: hyper-branched, polycarbonate, solid polymer electrolyte

References

[1] J.W. Fergus, Ceramic and polymeric solid electrolytes for lithium-ion batteries, J. Power Sources 195 (2010) 4554–4569, https://doi.org/10.1016/j.jpowsour.2010.01.076.

[2] M. Armand, J.M. Tarascon, Building better batteries, Nature 451 (2008) 652–657, doi:10.1038/451652a.

[3] J. Shim, D.-G. Kim, H.J. Kim, J.H. Lee, J.-C. Lee, Polymer composite electrolytes having core–shell silica fillers with anion-trapping boron moiety in the shell layer for all-solid-state lithium-ion batteries, ACS Appl. Mater. Interfaces 7 (2015) 7690–7701, doi: 10.1021/acsami.5b00618

[4] S.B. Peterson, J. Apt, J.F. Whitacre, Lithium-ion battery cell degradation resulting from realistic vehicle and vehicle-to-grid utilization, J. Power Sources 195 (2010) 2385–2392, https://doi.org/10.1016/j.jpowsour.2009.10.010.

[5] J.G. Kim, B. Son, S. Mukherjee, N. Schuppert, A. Bates, O. Kwon, M.J. Choi, H.Y. Chung, S. Park, A review of lithium and non-lithium based solid state batteries, J. Power Sources 282 (2015) 299–322, https://doi.org/10.1016/j.jpowsour.2015.02.054.

[6] D. Fenton, J. Parker, P. Wright, Complexes of alkali metal ions with poly(ethylene oxide), Polymer 14 (1973) 589, https://doi.org/10.1016/0032-3861(73)90146-8.

[7] A. Nishimoto, M. Watanabe, Y. Ikeda, S. Kohjiya, High ionic conductivity of new polymer electrolytes based on high molecular weight polyether comb polymers, Electrochim. Acta 43 (1998) 1177–1184, https://doi.org/10.1016/S0013-4686(97)10017-2.

[8] T. Itoh, S. Horii, T. Uno, M. Kubo, O. Yamamoto, Influence of hyperbranched polymer structure on ionic conductivity in composite polymer electrolytes of PEO/hyperbranched polymer/$BaTiO_3$/Li salt system, Electrochim. Acta 50 (2004) 271–274, https://doi.org/10.1016/j.electacta.2004.02.054.

[9] S.I. Lee, M. Schömer, H. Peng, K.A. Page, D. Wilms, H. Frey, C.L. Soles, D.Y. Yoon, Correlations between ion conductivity and polymer dynamics in hyperbranched

poly(ethylene oxide) electrolytes for lithium-ion batteries, Chem. Mater. 23 (2011) 2685–2688, https://doi.org/10.1021/cm103696g.

[10] C.J. Hawker, F. Chu, P.J. Pomery, D.J.T. Hill, Hyperbranched poly(ethylene glycol)s: a new class of ion-conducting materials, 29 (1996) 3831–3838, https://doi.org/10.1021/ma951909i.

[11] M. Ratner, D. Shriver, Ion transport in solvent-free polymers, Chem. Rev. 88 (1988) 109–124, https://doi.org/10.1021/cr00083a006.

[12] X. Wei, D.F. Shriver, Highly conductive polymer electrolytes containing rigid polymers, Chem. Mater. 10 (1998) 2307–2008, https://doi.org/10.1021/cm980170z.

[13] M.J. Smith, M.M. Silva, S. Cerqueira, J.R. MacCallum, Preparation and characterization of a lithium ion conducting electrolyte based on poly(trimethylene carbonate), Solid State Ion. 140 (2001) 345–351, https://doi.org/10.1016/S0167-2738(01)00815-3.

[14] B. Sun, J. Mindemark, K. Edström, D. Brandell, Polycarbonate-based solid polymer electrolytes for Li-ion batteries, Solid State Ion. 262 (2014) 738–742, https://doi.org/10.1016/j.ssi.2013.08.014.

[15] J. Mindemark, L. Imholt, J. Montero, D. Brandell, Allyl ethers as combined plasticizing and crosslinkable side groups in polycarbonate-based polymer electrolytes for solid-state Li batteries, J. Polym. Sci., Part A: Polym. Chem. 54 (2016) 2128–2135, https://doi.org/10.1002/pola.28080.

[16] J. Mindemark, L. Imholt, D. Brandell, Synthesis of high molecular flexibility polycarbonates for solid polymer electrolytes, Electrochim. Acta 175 (2015) 247–253, https://doi.org/10.1016/j.electacta.2015.01.074.

[17] T. Morioka, K. Ota, Y. Tominaga, Effect of oxyethylene side chains on ion-conductive properties of polycarbonate-based electrolytes, Polymer 84 (2016) 21–26, https://doi.org/10.1016/j.polymer.2015.12.036.

[18] Y. Tominaga, V. Nanthana, D. Tohyama, Ionic conduction in poly(ethylene carbonate)-

based rubbery electrolytes including lithium salts, Polym. J. 44 (2012) 1155–1158, https://doi.org/10.1038/pj.2012.97.

[19] Y. Tominaga, Ion-conductive polymer electrolytes based on poly(ethylene carbonate) and its derivatives, Polym. J. 49 (2017) 291–299, https://doi.org/10.1038/pj.2016.115.

[20] K. Kimura, J. Hassoun, S. Panero, B. Scrosati, Y. Tominaga, Electrochemical properties of a poly(ethylene carbonate)-LiTFSI electrolyte containing a pyrrolidinium-based ionic liquid, Ionics 21 (2015) 895–900, https://doi.org/10.1007/s11581-015-1370-x.

[21] V. Nanthana, Y. Tominaga, Synthesis and fundamental properties of carbon dioxide/alkylene oxide copolymers as ion-conductive polymers, Kobunshi Ronbunshu 70 (2013) 23–28, https://doi.org/10.1295/koron.70.23.

[22] M. Nakamura, Y. Tominaga, Utilization of carbon dioxide for polymer electrolytes [II]: Synthesis of alternating copolymers with glycidyl ethers as novel ion-conductive polymers, Electrochim. Acta 57 (2011) 36–39, https://doi.org/10.1016/j.electacta.2011.03.003.

[23] K. Matsumoto, T. Endo, K. Katsuda, H. Lee, K. Yamada, Synthesis of polycarbosilanes having a five-membered cyclic carbonate structure and their application to prepare gel polymer electrolytes for lithium ion batteries, J. Polym. Sci. Part A: Polym. Chem. 50 (2012) 5161–5169, https://doi.org/10.1002/pola.26359.

[24] K. Matsumoto, M. Kakehashi, H. Ouchi, M. Yuasa, T. Endo, Synthesis and properties of polycarbosilanes having 5-membered cyclic carbonate groups as solid polymer electrolytes, Macromolecules 49 (2016) 9441–9448, https://doi.org/10.1021/acs.macromol.6b01516.

[25] G. C. Behera, A. Saha, S. Ramakrishnan, Hyperbranched copolymers versus linear copolymers: a comparative study of thermal properties, Macromolecules 38 (2005) 7695–7701, https://doi.org/10.1021/ma0508146.

[26] Q. Zhu, J. Wu, C. Tu, Y. Shi, L. He, R. Wang, X. Zhu, D. Yan, Role of branching

architecture on the glass transition of hyperbranched polyethers, J. Phys. Chem. B 113 (2009) 5777–5780, https://doi.org/10.1021/jp900992e.

[27] E. Malmström, F. Liu, R.H. Boyd, A. Hult, U.W. Gedde, Relaxation processes in hyperbranched polyesters, Polym. Bull. 32 (1994) 679–685, https://doi.org/10.1007/BF00973919.

[28] J. Sun, K.I. Aly, D. Kuckling, A novel one-pot process for the preparation of linear and hyperbranched polycarbonates of various diols and triols using dimethyl carbonate, RSC Adv. 7 (2017) 12550–12560, https://doi.org/10.1039/C7RA01317E.

[29] H. Kudo, K. Maruyama, S. Shindo, T. Nishikubo, I. Nishimura, Syntheses and properties of hyperbranched polybenzoxazole by thermal cyclodehydration of hyperbranched poly[*o*-(*t*-butoxycarbonyl)amide] via A_2 + B_3 approach, J. Polym. Sci., Part A: Polym. Chem. 44 (2006) 3640–3649, https://doi.org/10.1002/pola.21449.

[30] M. Jikei, S.H. Chon, M. Kakimoto, S. Kawauchi, T. Imase, J. Watanabe, Synthesis of hyperbranched aromatic polyamide from aromatic diamines and trimesic acid, Macromolecules 32 (1999) 2061–2064, https://doi.org/10.1021/ma980771b.

[31] T. Emrick, H.T. Chang, J.M.J. Fréchet, An A_2 + B_3 approach to hyperbranched aliphatic polyethers containing chain end epoxy substituents, Macromolecules 32 (1999) 6380–6382, https://doi.org/10.1021/ma990687b.

[32] D. Yan, C. Gao, H. Frey, Hyperbranched Polymers; Wiley: New York, 2011; Chapter 3, 79, ISBN:978 0 471 78014 4.

[33] X. Chen, Z. Shen, Y. Zhang, New catalytic systems for the fixation of carbon dioxide. 1. Copolymerization of carbon dioxide and propylene oxide with new rare-earth catalysts-$RE(P_{204})_3$-Al(*i*-Bu)$_3$-$R(OH)_n$, Macromolecules 24 (1991) 5305–5308, https://doi.org/10.1021/ma00019a014.

[34] S. Selvasekarapandian, R. Baskaran, O. Kamishima, J. Kawamura, T. Hattori, Laser Raman and FTIR studies on Li^+ interaction in PVAc–$LiClO_4$ polymer electrolytes,

Spectrochim. Acta Part A 65 (2006) 1234–1240, https://doi.org/10.1016/j.saa.2006.02.026.

[35] P.G. Bruce, Solid State Electrochemistry, Cambridge University Press, Cambridge, 1995, 98-99. ISBN:0 521 40007 4.

[36] D.F. Shriver, B.L. Papke, M.A. Ratner, R. Dupon, T. Wong, M. Brodwin, Structure and ion transport in polymer-salt complexes, Solid State Ion. 5 (1981) 83–88, https://doi.org/10.1016/0167-2738(81)90199-5.

Scheme 1. a) Synthesis of a hyper-branched polycarbonate (HBPC) from dimethyl carbonate (DMC) and trimethylolethane (TME). b) Chemical structure of LPC.

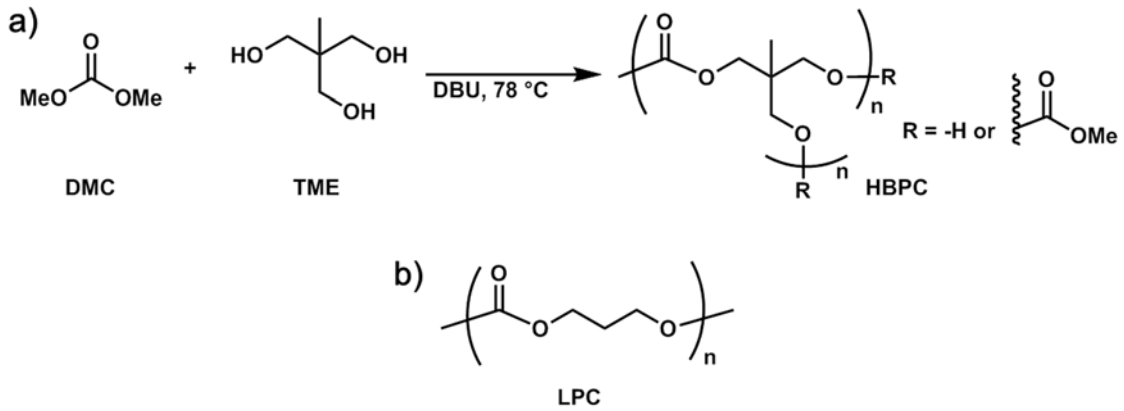

Fig. 1. GPC profile of obtained waxy solid (HBPC).

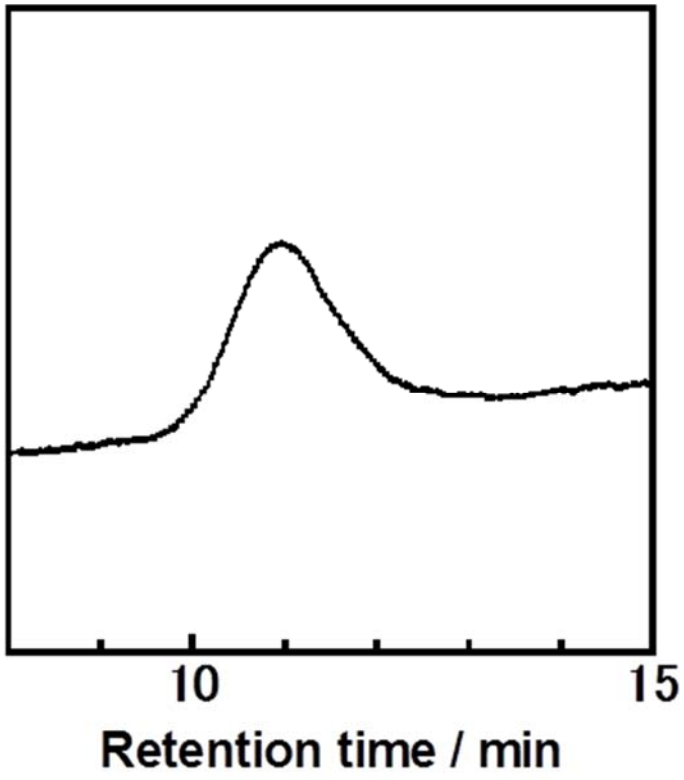

Fig. 2. a) ^{1}H and b) ^{13}C NMR spectra of HBPC in DMSO-d_6.

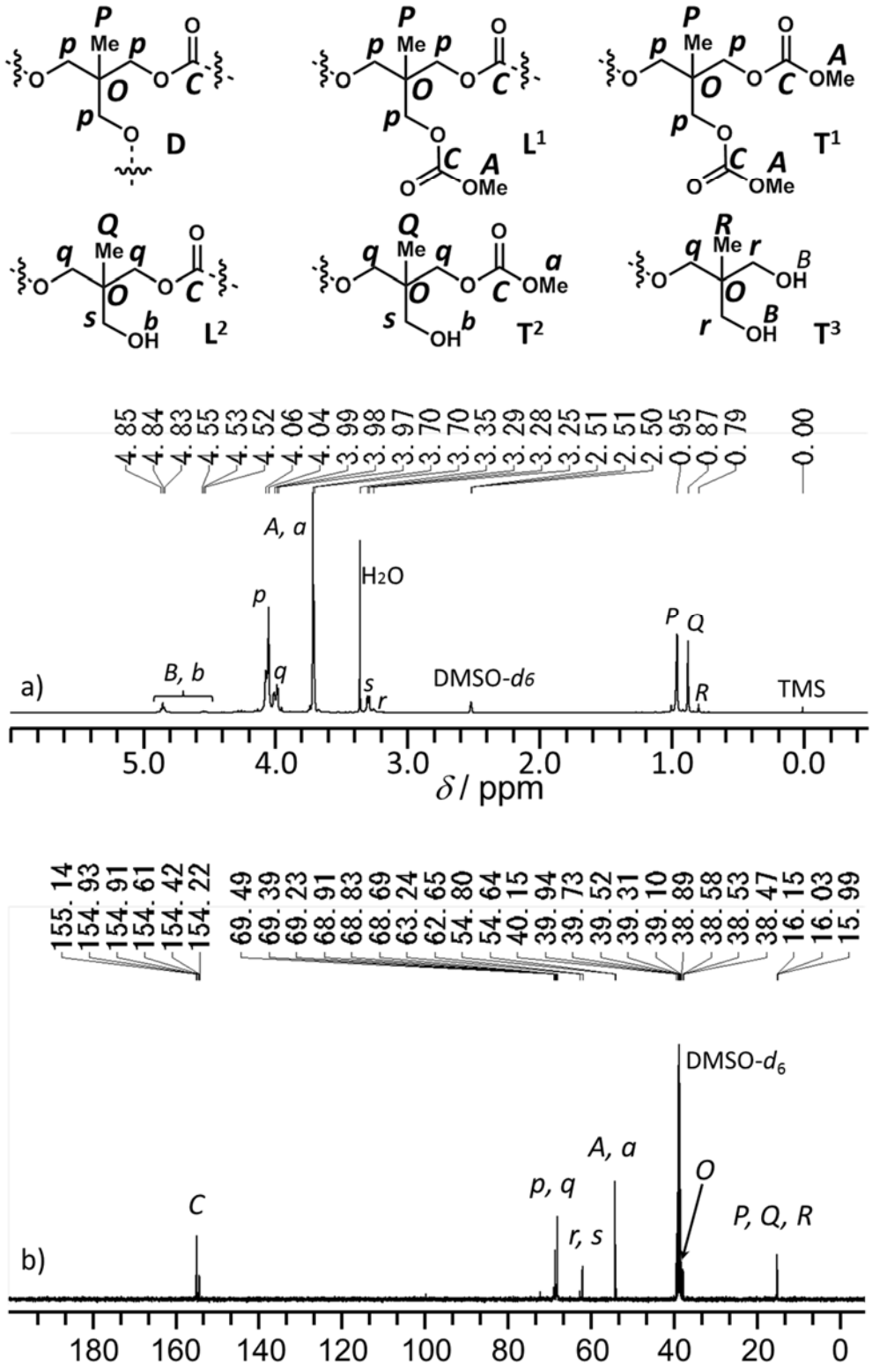

Fig. 3. Conversion of TME and mole compositions of three carbonate units against the reaction time. Equipped a) without (reflux conditions) and b) with a Dean-Stark receiver. Conversion of TME (○) and mole composition of tricarbonate unit (*P*, ●), dicarbonate unit (*Q*, ▲) and monocarbonate unit (*R*, ■).

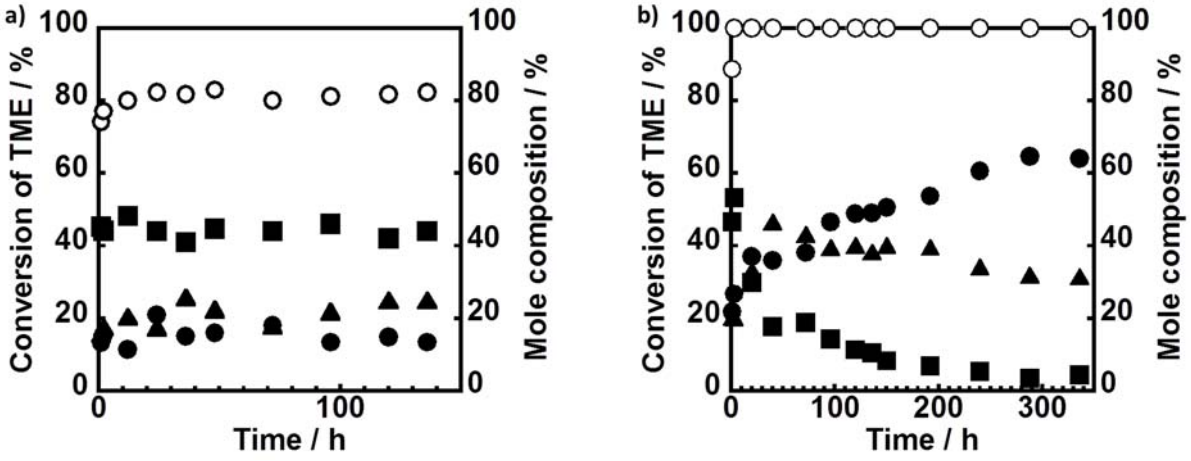

Fig. 4. Photographic images of HBPC-based SPE films. Added amounts of $LiClO_4$ are depicted according to the mole ratios of $LiClO_4$ to carbonate group ($[Li^+]$/[carbonate group]).

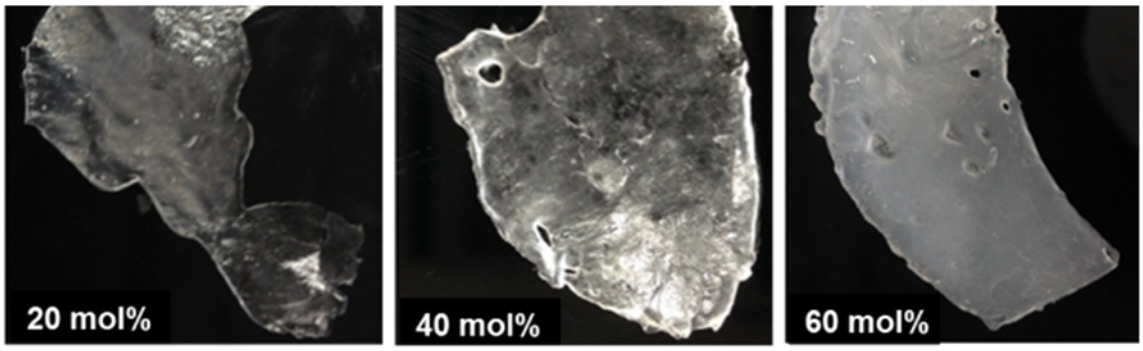

Fig. 5. a) DSC charts of HBPC and HBPC-based SPEs. b) FT-IR spectra of HBPC and SPEs. Added amounts of $LiClO_4$ are depicted according to the mole ratios of $LiClO_4$ to carbonate group ($[Li^+]$/[carbonate group]).

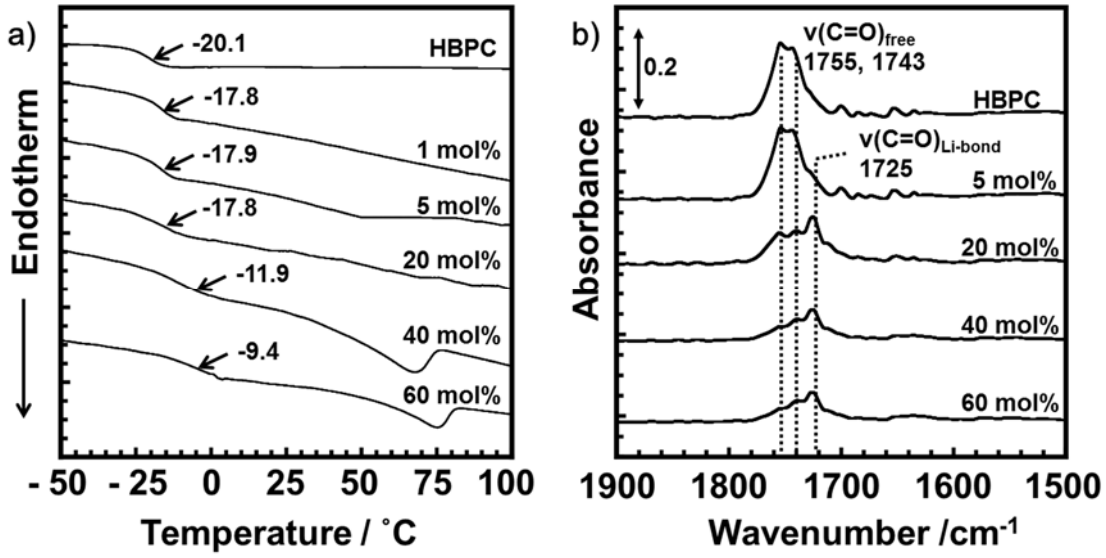

Fig. 6. a) Temperature dependence of the ion conductivities of HBPC-based and LPC-based SPEs. b) VTF plots of HBPC- and LPC-based SPEs containing $LiClO_4$. Added amounts of $LiClO_4$ are depicted according to the mole ratios of $LiClO_4$ to carbonate group ($[Li^+]$/[carbonate group]).

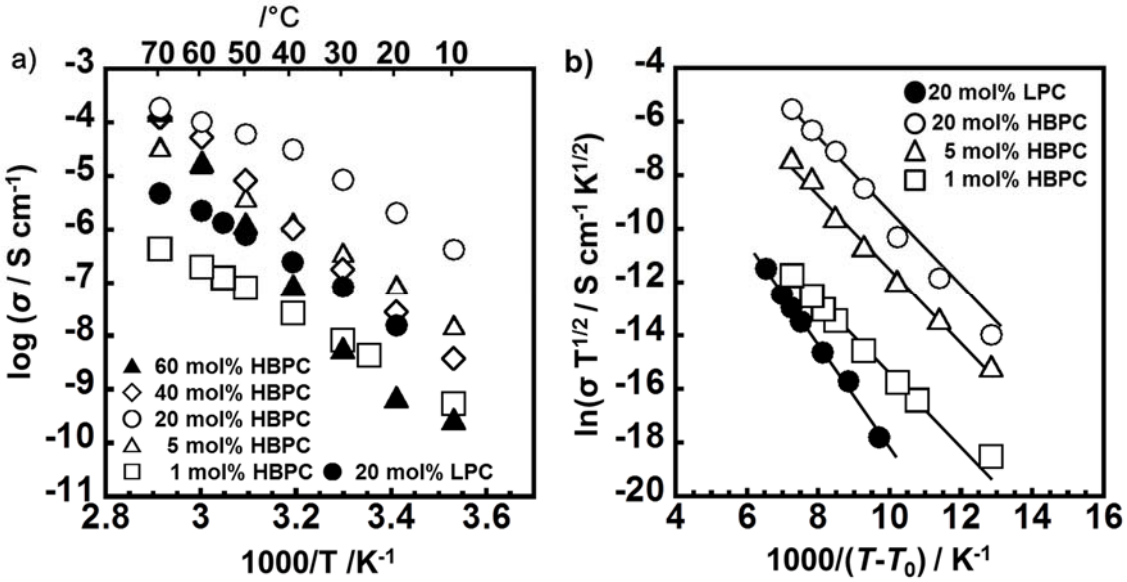

Table 1. 5% weight loss temperature (T_{d5}) of HBPC and HBPC-based SPEs.

[Li^+]/[carbonate group] mol%	T_{d5} / °C
0	163.5
1	189.3
5	188.3
20	174.4
40	178.3
60	177.2

Supporting Information (SI)

Synthesis of an Aliphatic Hyper-branched Polycarbonate and Determination of its Physical Properties for Solid Polymer Electrolyte Use

Suguru Motokucho, Hirotoshi Yamada, Yusuke Suga, Hiroshi Morikawa, Hisayuki Nakatani, Kouki Urita, Isamu Moriguchi

Fig. S1. ^{1}H NMR spectrum of the reaction mixture of TME and DMC in DMSO-d_6.